Structural, Chemical, and Transport Properties of a New Clathrate Compound: $Cs_8Zn_4Sn_{42}$

G. S. Nolas*

R & D Division, Marlow Industries, Inc., 10451 Vista Park Road, Dallas, Texas 75238

T. J. R. Weakley

Department of Chemistry, University of Oregon, Eugene, Oregon 97403

J. L. Cohn

Department of Physics, University of Miami, Coral Gables, Florida 33124

Received March 19, 1999. Revised Manuscript Received June 30, 1999

The synthesis and structural, chemical, and transport properties of a new clathrate compound with elemental composition $Cs_8Zn_4Sn_{42}$ is reported. This compound is cubic with space group $Pm\bar{3}n$ and a lattice parameter of 12.1226(19) Å. Single-crystal X-ray diffraction and structural refinement indicate that Cs atoms reside in the polyhedral cavities formed by the tetrahedrally bonded network of Zn and Sn atoms. The Cs atom in the larger polyhedra (tetrakaidecahedra) exhibit greater and more anisotropic thermal motion than those of the smaller polyhedra (dodecahedra). This "rattling" of the Cs contributes to the low thermal conductivity of this compound, obtained on a polycrystalline pellet. In addition, Zn is ordered in this compound. Electronic properties and the potential of this type of Sn-clathrate for thermoelectric applications are also discussed.

Introduction

Semiconducting compounds with a clathrate hydrate-type crystal structure are of growing interest since their transport properties and wide band gap show promise for thermoelectric[1−3] and optical applications,[4] respectively. These "open structured" materials possess a framework with large polyhedral "cages" in the crystal lattice which can incorporate "guest" atoms. Semiconductor compounds with this type of crystal structure possess low thermal conductivity values, approaching values typical of amorphous materials, a prerequisite for thermoelectric applications.[1−3] Theoretical calculations indicate that these compounds may possess a wide band gap, as compared to the diamond structure, due to the altered bonding geometry.[4] This approach is somewhat similar to that for porous silicon.[5]

The two most well-known of the clathrate hydrate crystal structures are those of type-I (e.g., $(CH_4)_8(H_2O)_{46}$) and type-II (e.g., $(C_3H_8)_{24}(H_2O)_{136}$).[6] Cros and coworkers[7] were first to identify the analogous silicon compounds, Na_8Si_{46} and Na_xSi_{136}, respectively, where x can be a maximum of 24. The framework in these compounds is formed by covalent tetrahedrally bonded atoms, Si for example, comprised of two different face-sharing polyhedra that are connected to each other by these shared faces. The type-I structure contains 2 pentagonal dodecahedra and 6 tetrakaidecahedra (12 pentagonal and 2 hexagonal faces) per cubic unit cell. The type-II structure contains 16 pentagonal dodecahedra and 8 hexakaidecahedra (12 pentagonal and 4 hexagonal faces) per cubic unit cell. The very low thermal conductivity measured in compounds with this crystal structure (for clathrate hydrates[8] as well as Si-, Ge-, and Sn-clathrates[1−3]) is due to guest−host interactions whereby the localized guest vibrations interact strongly with the host acoustic modes. The guest translational vibration (or "rattling") frequencies increase as the size difference between guest and host polyhedra decreases as a result of the stronger restoring forces of the guest atom.[2]

With few exceptions[2,3] most of the work thus far on the transport properties of these types of compounds has focused on Si or Ge as the framework atoms. However there has been work reported on the synthesis and crystal structure of Sn-clathrate compounds. Table 1 lists these compounds, to the best of our knowledge, from the literature along with some structural data.[15]

(1) Nolas, G. S.; Cohn, J. L.; Slack, G. A.; Schujman, S. B. *Appl. Phys. Lett.* **1998**, *73*, 178−180.
(2) Cohn, J. L.; Nolas, G. S.; Fessatidis, V.; Metcalf, T. H.; Slack, G. A. *Phys. Rev. Lett.* **1999**, *82*, 779−782.
(3) Nolas, G. S. In *Thermoelectric Materials−The Next Generation Materials for Small-Scale Refrigeration and Power Generation Applications*; Tritt, T. M., Mahan, G., H. B. Lyon, H. B., Jr., Kanatzidis, M.G., Eds.; Mater. Res. Soc. Symp. Proc. Vol. 545; Materials Research Society: Pittsburgh, PA, 1999; pp 435−442.
(4) Adams, G. B.; O'Keeffe, M.; Demkov, A. A.; Sankey, O. F.; Huang, Y. *Phys. Rev. B* **1994**, *49*, 8048−8053, and references therein.
(5) Canham, L. T. *Phys. Rev. Lett.* **1990**, *57*, 1046−1049.
(6) See for example: Franks, F. *Water, A Comprehensive Treatise*; Plenum Press: New York, 1973.
(7) Cros, C.; Pouchard, M.; Hagenmuller, P. *C. R. Acad. Sci.* **1965**, *260*, 4764−4767.
(8) Tse, J. S.; White, M. A. *J. Phys. Chem.* **1988**, *92*, 5006−5011.
(9) Zhao, J.-T.; Corbett, J. D. *Inorg. Chem.* **1994**, *33*, 5721−5726.
(10) Gallmeier, G.; Schafter, H.; Weiss, A. *Z. Naturforsch.* **1969**, *B24*, 665−667.

10.1021/cm990164i CCC: $18.00
Published on Web 09/01/1999

Table 1. Crystal Structure, Room Temperature Lattice Parameter (a_o) and References to These Sn-Clathrate Compounds

compound	crystal structure	a_o (Å)	ref(s)
M_8Sn_{44}	$Pm\bar{3}n$	12.054[a]	2,3,9
$K_{1.6}Cs_{6.4}Sn_{44}$	$Pm\bar{3}n$	12.084	9
K_8Sn_{46}	$Pm\bar{3}n$	12.030	10
$M_8Z_8Sn_{38}$	$Pm\bar{3}n$	11.974[b]	3,11,12
$K_8Z_{23}Sn_{23}$	$Pm\bar{3}n$	11.962[c]	13
$Ba_{16}Ga_{32}Sn_{104}$	$Fd\bar{3}m$	17.054	14

[a] Rb_8Sn_{44}. [b] $Rb_8Ga_8Sn_{38}$. [c] $K_8Ga_{23}Sn_{23}$.

The compounds M_8Sn_{44} (where M is an alkali metal atom) and $K_{1.6}Cs_{6.4}Sn_{44}$ are defect members of the type-I clathrates with two anion vacancies per formula unit at the 6*c* crystallographic positions. The set of compounds K_8Sn_{46}, $M_8Ga_8Sn_{38}$, and $K_8Z_{23}Sn_{23}$ (where Z = Al, Ga, and In) have the type-I clathrate crystal structure. The $Ba_{16}Ga_{32}Sn_{104}$ compound has the type-II structure.

In this work, we present the results of an investigation of a new type-I Sn-clathrate compound, $Cs_8Zn_4Sn_{42}$. The Cs atoms reside in the cages of the three-dimensional network of tetrahedrally bonded Zn and Sn atoms. We present refinement of the site occupancies of the constituents and low-temperature transport measurements with the aim of illustrating the correlation between the structural data and the thermal conductivity measurements. We also discuss the potential of this type of material system for thermoelectric applications.

Sample Preparation

Small crystals of $Cs_8Zn_4Sn_{42}$ were synthesized as follows. High purity elements were mixed in an argon atmosphere glovebox and reacted for two weeks at 550 °C inside a tungsten crucible which was itself sealed inside a stainless steel canister. The canister was evacuated and back-filled with high purity argon gas before sealing. The resulting compound consisted of small octahedrally shaped crystals with a shiny, somewhat blackish, metallic luster. These millimeter-sized crystals were not reactive in air or moisture. For transport measurements these crystals were ground to fine powders and hot pressed inside a graphite die at 380 °C and 20 500 lbs/in^2 for 2 h in an argon atmosphere. The resulting pellet had a density of 5.56 g/cm^3, or about 95% of theoretical density. Electron-beam microprobe analysis of the polished surface revealed the exact stoichiometry of the phase-pure compound.

Results and Discussion

Structural Details. The smaller of the single crystals of $Cs_8Zn_4Sn_{42}$ were isolated and investigated employing an Enraf-Nonius CAD-4 single-crystal diffractometer with graphite monochromator and Mo Kα radiation. The Laue symmetry *m*3*m* was confirmed by the measurement of potential equivalents for several reflections. Table 2 contains a summary of crystal data, data collection, structural refinement, and the final residuals. The structural refinement confirms the assignment of the space group $Pm\bar{3}n$ (no. 223), corresponding to the type-I clathrate structure, on the basis of the systematic absences. Absorption corrections based on azimuthal scans (ψ) were applied. A SIR92 E-map[18] showed five independent atoms, which were identified as Cs or Sn on the basis of coordination numbers and bond lengths. Refinement of occupancy factors for the three independent Sn atoms showed that the four Zn atoms per unit cell were randomized at the 6*c* [Sn(1)] sites. The TEXSAN program suite,[19] incorporating complex atomic scattering factors, was used in all calculations.

Table 2. Details of the X-ray Data Collection and Structural Refinements of Cubic $Cs_8Zn_4Sn_{42}$ Obtained at a Temperature of 22 °C

space group	$Pm\bar{3}n$
lattice parameter, a_o (Å)	12.1226(19)
formula units/cell, Z	1
formula weight	6043.9
calculated density (g/cm^3)	5.633
crystal dimensions (mm)	0.02 × 0.03 × 0.07
radiation	Mo Kα, 0.71073 Å
maximum 2θ	60°
F_{000}	2550
index range *h*, *k*, *l*	0→17, 0→9, 0→11
total number of reflections	495
no. of unique reflections	495
absorption Correction	azimuthal
relative correction factors	0.68−1.00
2nd extinction parameter, g	2.0(2) × 10^{-7}
reflections with $I \geq 1.5\sigma(I)$	308
no. of parameters, V	19
function minimized	$\sum w(\lvert F_o \rvert - \lvert F_c \rvert)^2$
conventional residual, *R*	0.059
weighted residual, wR	0.050
weighting factor, *w*	$1/\sigma^2(F)$
goodness of fit, *S*	1.41

Figure 1 is a schematic of the crystal structure of $Cs_8Zn_4Sn_{42}$ drawn using the structural analysis obtained from the crystal X-ray data. The (Sn,Zn) framework atoms form bonds to each other in a distorted tetrahedral arrangement. These framework atoms form polyhedra with shared faces. As stated above there are eight polyhedra per cubic unit cell, Sn_{20} dodecahedron, and $(Zn,Sn)_{24}$ tetrakaidecahedron in a 1:3 ratio, respectively. The Cs atoms reside inside these polyhedra, at the 2*a* and 6*b* crystallographic positions, respectively. Due to this encapsulation of the Cs atoms $Cs_8Zn_4Sn_{42}$ is stable in air and moisture, unlike CsSn.

The specific framework and thermal parameters are an important aspect of this structure. These properties have an affect on the transport properties, as will be discussed below. One of the more interesting structural features is the asymmetry of the Cs(2) thermal motion (U_{ij}). This is illustrated in Figure 2 and tabulated in Table 3. Note the difference in the thermal ellipsoids between the Cs(2) atoms and the Cs(1) atoms. The Cs-

(11) Kröner, R.; Peters, K.; von Schnering, H. G.; Nesper, R. *Z. Kristallogr.* **1998**, *213*, 667−668; 671−672; 675−676.
(12) von Schnering, H. G.; Kröner, R.; Menke, H.; Peters, K.; Nesper, R. *Z. Kristallogr.* **1998**, *213*, 677−678.
(13) Westerhaus, W.; Schuster, H. *Z. Natruforsch* **1977**, *B32*, 1365−1367.
(14) Kröner, R.; Nesper, R.; von Schnering, H. G. *Z. Kristallogr.* **1989**, *186*, 172.
(15) The compounds K_8Sn_{25} and $K_6Sn_{23}Bi_2$ contain dodecahedral cages with K residing inside.[9,16] The compound $Ba_8Ga_{16}Sn_{30}$ does not synthesize into the type-I clathrate structure although it has a similar chemical formula.[3,17] The (Ga,Sn) atoms are however tetrahedrally coordinated as in the case of the type-I clathrate structure and enclose the Ba atom inside.
(16) Fassler, T. F. *Z. Anorg. Allog. Chem.* **1998**, *624*, 569−577.
(17) Eisenmann, B.; Schafer, H.; Zagler, R. *J. Less-Common Met.* **1986**, *118*, 43−55.
(18) Altomare, A.; Cacarano, G.; Giacovazzo, C.; Guagliardi, A.; Burla, M. C.; Polidori, G.; Camalli, N. *J. Appl. Crystallogr.* **1994**, *27*, 435.
(19) TeXsan Software for Single-Crystal Structure Analysis, version 1.7; Molecular Structures Corporation: The Woodlands, TX 77381.

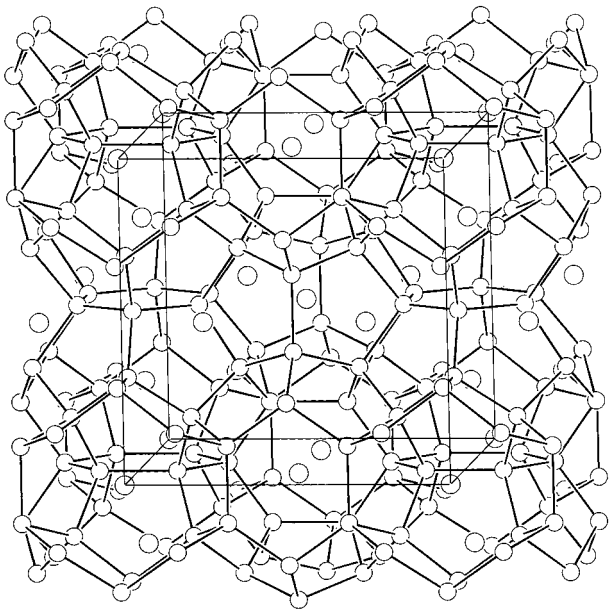

Figure 1. Crystal structure of $Cs_8Zn_4Sn_{42}$.

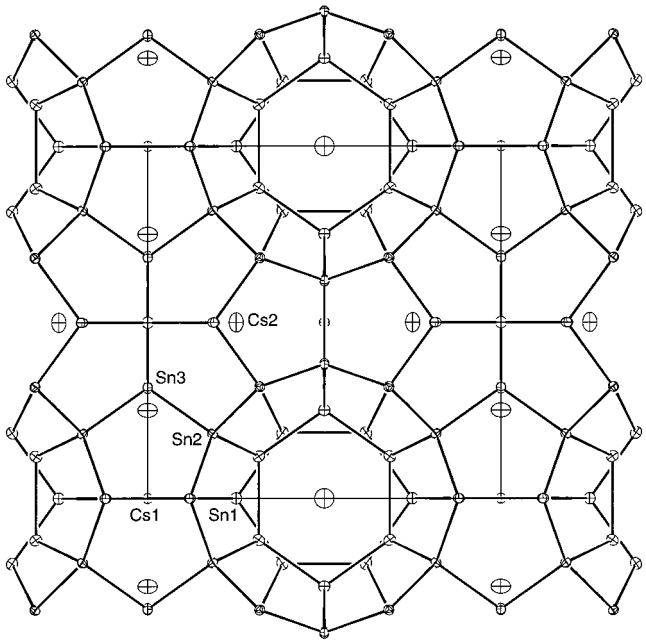

Figure 2. Graphical illustration of the crystal structure of $Cs_8Zn_4Sn_{42}$ along (100) showing the thermal ellipsoids of the constituent elements.

(1) atoms have nearly symmetric thermal motions that are similar in magnitude to that of the (Zn,Sn) framework atoms. The Cs(2) atom displacements U_{22} and U_{33} are 3−4 times larger than those of the other constituent atoms. This is typical of compounds with this type of crystal structure[20] and may be the source of substantial phonon scattering that is implied by the relatively low thermal conductivity in this compound.

Table 4 lists the interatomic bond lengths and some bond angles of $Cs_8Zn_4Sn_{42}$. Note in the case of the Sn(1) positions this also includes Zn(1). The Sn−Sn−Sn bond angles range from 106 to 125°. The Sn−Sn bond lengths are similar to that for gray-Sn (the diamond structured α-Sn) with 2.8099 Å. From Table 4, we can estimate the average cage size of the Sn_{20} dodecahedra and $(Zn,Sn)_{24}$ tetrakaidecahedra, assuming the shortest interatomic distances. These are 2.44 and 2.64 Å, respectively.

Transport Measurements. The hot-pressed pellet was cut with a wire-saw in the shape of a parallelpiped $2 \times 2 \times 5$ mm^3 in size. Four-probe electrical resistivity (ρ), steady-state Seebeck coefficient (S), and steady-state thermal conductivity measurements were performed in a radiation-shielded vacuum probe with the heat flow measured along the longest axis. Heat losses via conduction through the lead wires and radiation were determined in separate experiments and the data corrected accordingly. These corrections were ∼15% at room temperature and <5% below 120 K.

Figure 3 shows ρ and S as a function of temperature for a hot-pressed polycrystalline $Cs_8Zn_4Sn_{42}$ sample from 300 to 5 K. The nonmonotonic $\rho(T)$ behavior is indicative of multiband conduction, with differing temperature-dependent mobilities. The negative sign of S indicates that the majority carriers are electrons. However, for T >100 K, both transport coefficients exhibit an activated behavior with a small characteristic energy, estimated to be 330 K from the slope of S plotted against $1/T$. The curvature of $S(T)$ in this temperature range suggests that this activated behavior is associated with holes. That $S < 0$ at low T suggests impurity-band conduction by electron donors. The decrease in ρ at $T <$ 100K presumably reflects the increasing mobility of these donors with decreasing temperature. A small activation energy (<25 K) is inferred from the rise in ρ and change in sign of S from negative to positive below 13 K.

From the measured values of κ and ρ, and the Wiedemann−Franz law (with ideal Lorenz number, $L_o = 2.44 \times 10^{-8}$ V^2/deg^2) we can estimate the lattice component of the thermal conductivity, $\kappa_g = \kappa - L_oT/\rho$. Figure 4 shows κ_g of polycrystalline $Cs_8Zn_4Sn_{42}$ in the temperature range of 300−6 K. Also in this figure are κ_g data for Cs_8Sn_{44} and $Sr_8Ga_{16}Ge_{30}$ polycrystalline samples.[1,2] The electronic component of the thermal conductivity, $\kappa_e = L_oT/\rho$, for $Cs_8Zn_4Sn_{42}$ is <2% of the total thermal conductivity in the temperature range investigated.

The Cs_8Sn_{44} compound exhibits a temperature-dependent κ_g which is typical of simple crystalline insulators, with κ_g increasing with decreasing temperature approximately as $1/T$, the signature of propagating phonons scattered by anharmonic interactions. In the case of the $Cs_8Zn_4Sn_{42}$ compound, κ_g also increases with decreasing T, however not as strongly, indicating additional phonon scattering mechanisms present. Reitveld refinement on powdered Cs_8Sn_{44} indicates that the thermal ellipsoids of the Cs atoms are similar in shape to those of the $Cs_8Zn_4Sn_{42}$ compound; however, the mean-square displacements of Cs(2) in the former are not as large. The two Sn vacancies per unit cell in Cs_8Sn_{44} are on the Sn(1) site, and additional bonding induced between Cs and Sn atoms neighboring the vacancies may constrain the Cs(2) displacements. This structural difference between the two compounds may be the source of their differing low-T thermal conductivities. The localized vibrations, or "rattling", of Cs(2) in $Cs_8Zn_4Sn_{42}$ couple to the heat-carrying phonons producing resonant damping of these phonons. We note

(20) Nolas, G. S.; Weakley, T. J. R. Unpublished results.

Table 3. Atomic Parameters of $Cs_8Zn_4Sn_{42}$[a]

atom	Cs(1)	Cs(2)	Sn(1)	Sn(2)	Sn(3)
site	2a	6d	6c	16i	24k
x	0.0000	0.2500	0.2500	0.18309(9)	0.0000
y	0.0000	0.5000	0.0000	0.1831	0.341429(15)
z	0.0000	0.000	0.5000	0.1831	0.11878(15)
U_{11} (Å^2)	0.0128(12)	0.025(3)	0.016(3)	0.0125(5)	0.0114(9)
U_{22} (Å^2)	0.0128	0.047(2)	0.0163(18)	0.0125	0.0170(9)
U_{33} (Å^2)	0.0128	0.0472	0.0163	0.0125	0.0154(9)
U_{12} (Å^2)	0.0000	0.0000	0.0000	−0.0007(4)	0.0000
U_{13} (Å^2)	0.0000	0.0000	0.0000	−0.0007	0.0000
U_{23} (Å^2)	0.0000	0.0000	0.0000	−0.0007	0.0022(9)
B_{eq} (Å^2)	1.008(16)	3.15(6)	1.26(6)	0.990(7)	1.15(4)

[a] The anisotropic thermal parameters are defined by $T = \exp(-2\pi^2\sum_i\sum_j U_{i\ j} h_i h_j a^*_i a^*_j)$. The equivalent isotropic thermal parameter is defined by $B_{eq} = (8\pi^2/3)\sum_i\sum_j U_{i\ j}\ a^*_i a^*_j a_i a_j$).

Table 4. Interatomic Bond Lengths[a] (Å) and Bond Angles (deg) in $Cs_8Zn_4Sn_{42}$

Cs(1)−Sn(2)	3.844(2)	Sn(1)−Sn(3i)	2.757(2)
Cs(1)−Sn(3)	4.073(2)	Sn(2)−Sn(2ii)	2.810(4)
Cs(2)−Sn(1i)	4.2860(3)	Sn(2)−Sn(3)	2.840(1)
Cs(2)−Sn(2)	4.5104(6)	Sn(3)−Sn(3iii)	2.880(4)
Cs(2)−Sn(3)	4.041(1)		
Sn(3)−Sn(1)-Sn(3)	109.45(4)	Sn(1)−Sn(3)-Sn(2)	107.40(6)
Sn(3)−Sn(1)-Sn(3)	109.51(7)	Sn(1)−Sn(3)-Sn(3)	125.25(4)
Sn(2)−Sn(2)-Sn(3)	106.64(5)	Sn(2)−Sn(3)-Sn(2)	102.82(7)
Sn(3)−Sn(2)-Sn(3)	112.15(4)	Sn(2)−Sn(3)-Sn(3)	105.94(4)

[a] Symmetry code: (i) *z*, *y*, *x*; (ii) $^1/_2 - x$, $^1/_2 - z$, $^1/_2 - y$; (iii) $-x$, *y*, $-z$.

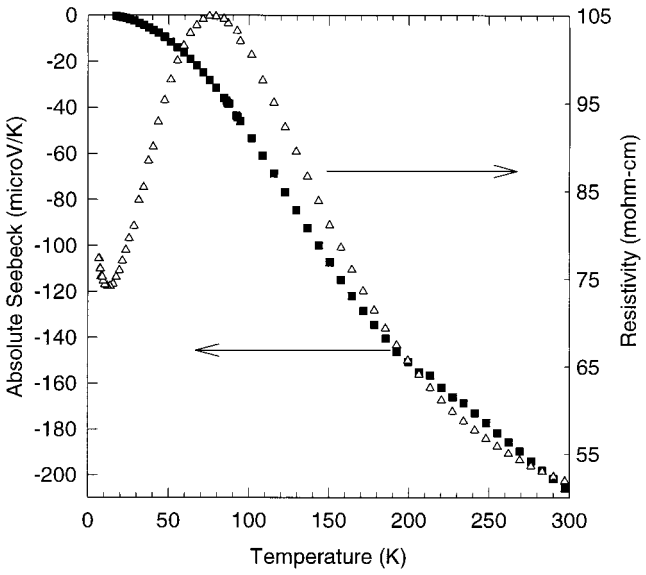

Figure 3. Resistivity (open triangles) and Seebeck coefficient (closed circles) as a function of temperature for $Cs_8Zn_4Sn_{42}$.

the measured grain size of polycrystalline $Cs_8Zn_4Sn_{42}$ (11 μm) is approximately the same as that of the polycrystalline Cs_8Sn_{44} compound[2] shown in Figure 4 (13 μm) and thus differences in grain-boundary scattering cannot explain the κ_g difference between these two compounds. Sn vacancies may produce Rayleigh scattering,[21] which may account for the lower room-temperature value of κ_g in Cs_8Sn_{44}. While the enhanced thermal motion of the Cs(2) atoms in $Cs_8Zn_4Sn_{42}$ appears to diminish κ_g, the effect is not as great as that caused by Sr(2) motion in $Sr_8Ga_{16}Ge_{30}$ (Figure 4)—there the Sr(2) thermal ellipsoids are nearly an order of magnitude larger than those of the (Ga,Ge) framework

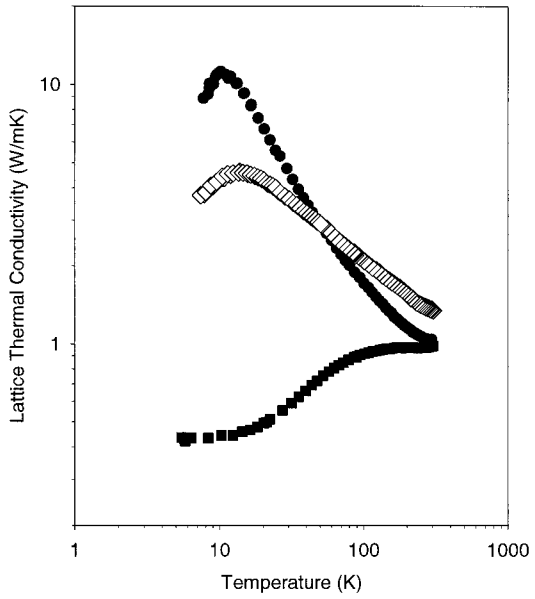

Figure 4. Lattice thermal conductivity versus temperature for $Cs_8Zn_4Sn_{42}$ (open squares), Cs_8Sn_{44} (filled circles), and $Sr_8Ga_{16}Ge_{30}$ (filled squares).

atoms. The structural refinement of this latter compound will be presented in a future article.

Conclusions

We report on the synthesis, structural, and transport properties of a new compound with the type-I clathrate hydrate crystal structure. As is typical of compounds with this crystal structure the "guest" atoms in the larger tetrakaidecahedra cages have larger, anisotropic thermal ellipsoids as compared to that of the smaller dodecahedra cages. Although κ_g of this sample is rather low the temperature dependence is typical of imperfect crystalline semiconductors, unlike the glasslike behavior observed for Ge-clathrates. In addition this compound most likely has a very small band gap, if nonzero. This, along with the fact that the Seebeck coefficient is relatively high, makes these materials rather interesting for thermoelectric cooling applications. Although a relatively low thermal conductivity has been measured in $Cs_8Zn_4Sn_{42}$, and in $Rb_8Ga_8Sn_{38}$ with $\kappa_g \sim 1$W/mK at room temperature,[3] these types of compounds will find use as thermoelectric materials only if the thermal conductivity is further reduced.

(21) Abeles, B. *Phys. Rev.* **1963**, *131*, 1906−1911.

CM990164I